

An infrared reporter to detect spatiotemporal dynamics of protein-protein interactions

Emmanuelle Tchekanda, Durga Sivanesan & Stephen W Michnick

We report a protein-fragment complementation assay (PCA) based on the engineered *Deinococcus radiodurans* infrared fluorescent protein IFP1.4. Unlike previous fluorescent protein PCAs, the IFP PCA is reversible, allowing analysis of spatiotemporal dynamics of hormone-induced signaling complexes in living yeast and mammalian cells at nanometer resolution. The inherently low background of infrared fluorescence permitted detection of subcellular reorganization of a signaling complex expressed at low abundance.

PCAs based on fluorescent protein reporters are popular methods for visualizing protein-protein interactions (PPIs)^{1,2}. However, such PCAs are irreversible, a limitation that prevents meaningful study of PPI spatiotemporal dynamics³. The principle of PCA is that complementary N- and C-terminal fragments are genetically fused to coding sequences of two proteins of interest. The fusions are expressed in any cell type, and if the two proteins interact, they bring together the two PCA reporter protein fragments, which can then fold, reconstituting the proteins' activity^{4,5}. All PCAs tested are reversible except those based on fluorescent proteins^{6–8}.

All PCA reporter proteins, except for fluorescent proteins, are formed of subdomains associated through weak interactions⁹. These weak interdomain contacts render these proteins susceptible to destabilization, such as would occur when interacting proteins dissociate in a PCA, resulting in spontaneous unfolding of the PCA reporters, as we have observed for all cases studied^{6–8}.

We postulated that a reversible PCA could be developed from the monomeric IFP1.4, the engineered chromophore-binding domain (CBD) of a bacteriophytochrome from *D. radiodurans*^{10,11}. A PCA based on a related fluorescent protein (iRFP) was recently reported, but it was irreversible and dimeric, thereby preventing its application to measurement of spatiotemporal dynamics or complex stoichiometry¹². The topology of the CBD contains a figure-eight knot between N-terminal PAS (Per/Arndt/Sim) and C-terminal GAF (cGMP phosphodiesterase/adenyl cyclase/FhlA) subdomains. GAF forms most of the chromophore-binding

pocket¹¹ (Fig. 1a,b). The chromophore, biliverdin, forms a covalent adduct with Cys24 on the PAS domain, resulting in mature fluorescent holoprotein¹¹ (Fig. 1b).

Integrity of the knot is necessary for stability of the GAF domain and chromophore binding¹³. Thus, we dissected IFP1.4 at 13 sites, as far from the knot as possible (Fig. 1a). We constructed *Escherichia coli* expression plasmids encoding IFP1.4 N- and C-fragment pairs fused 3' to the coding sequence of homodimerizing GCN4 leucine zippers (Zip; residues 250–281) via a flexible peptide linker ((Gly₄Ser)₂) under the arabinose-inducible *araB* promoter (Supplementary Tables 1 and 2). We sequentially cotransformed *E. coli* BL21-DE3 cells with pairs of complementary fragment-encoding plasmids and selected individual clones to test fluorescence (Online Methods). The best results were obtained for fragments dissected between residues 132 and 133, located at approximately equal distances from the knot and biliverdin-binding site (Supplementary Fig. 1a,b and Supplementary Table 3). All further experiments were performed with these fragments, henceforth referred to as IFP-F[1] and IFP-F[2], respectively.

We compared the fluorometric properties of the IFP PCA to native IFP1.4 both *in vitro* and *in vivo* (Fig. 1c–f). We expressed and purified Zip-IFP-F[1] and Zip-IFP-F[2] from *E. coli* and performed fluorescence spectroscopy in the presence of biliverdin (4 μg ml⁻¹) (Fig. 1d). We determined the extinction coefficient on the assumption that absorbance of the IFP PCA at 388 nm was due to bound biliverdin and therefore equal to that of the free chromophore¹⁰. We measured an extinction coefficient of ~42,890 M⁻¹ cm⁻¹ for the IFP PCA, compared to 92,000 M⁻¹ cm⁻¹ for full-length IFP1.4. The quantum yield of the IFP PCA was 0.068, compared to full-length IFP1.4 of 0.07 (Online Methods)¹⁰. Surprisingly, the IFP PCA retained approximately 50% of the fluorescence brightness of full-length IFP1.4, with identical excitation and emission maxima¹⁰ (Fig. 1e and Supplementary Table 4).

We tested the IFP PCA with known interactions including protein kinase PKA subunits (Tpk2-Bcy1); a homodimerizing zipper; the FKBP12 mutant F_{M1}, which interacts with itself; and a mutant of the protein Ypd1 (Trp80-Ala, Ypd1*) that binds to Ssk1t but not to Skn7t. As predicted, the Ssk1t-Ypd1* complex was detectable by the IFP PCA, but the Skn7t-Ypd1* interaction was not (Fig. 1f).

We further used the Ssk1t-Ypd1* and Skn7t-Ypd1* pairs to test for concentration-dependent folding of PCA fragments in the absence of a PPI¹⁴. We expressed Skn7t-IFP-F[1] and Ypd1*-IFP-F[2] pairs under *GAL*, *ADH*, *TEF* and *GPD* promoters that drive expression of up to 10⁵ protein copies of the genes that they control per cell¹⁵ (Fig. 1g). No IFP PCA signal was detectable for Skn7t-Ypd1* expressed up to the highest natural levels.

We next tested the capacity of the IFP PCA to distinguish PPIs with different dissociation constants (*K_D*) using mutants of the Ras-binding domain of Raf (RBD) with known *K_D* values for Ras¹⁶

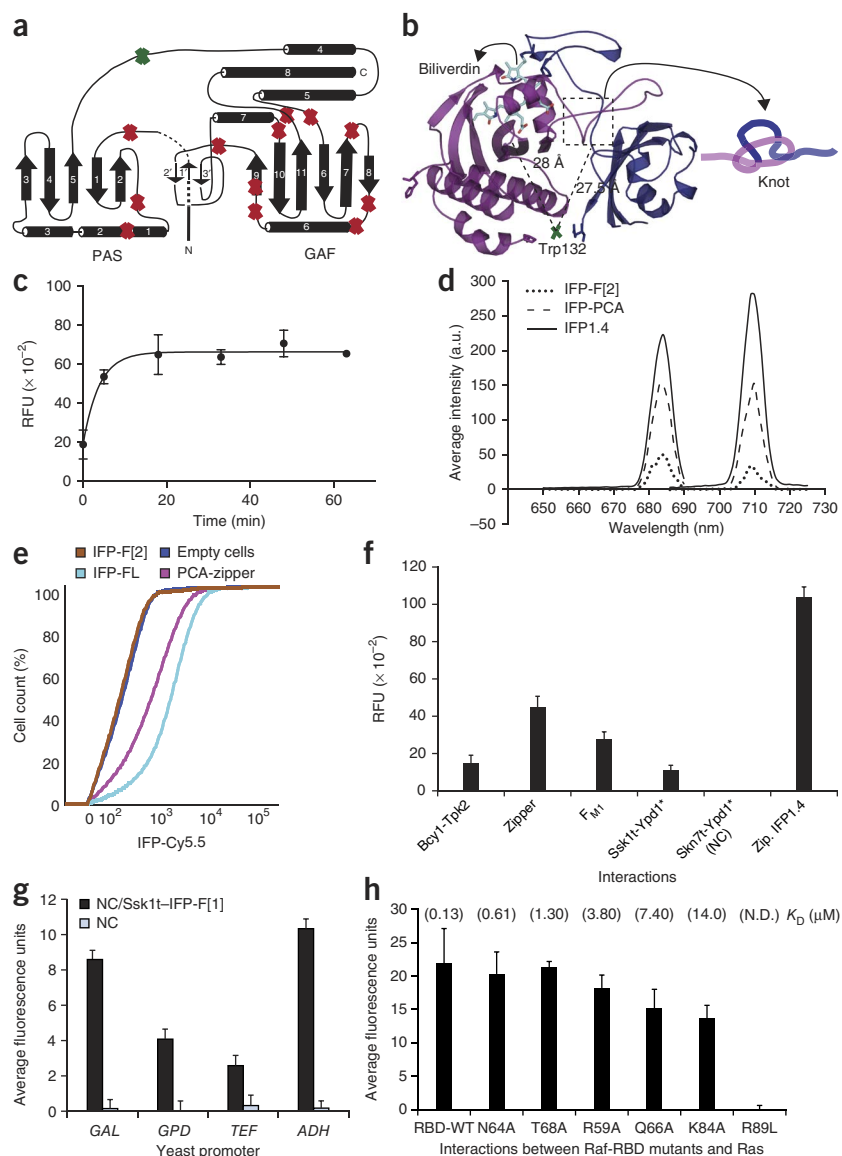
Figure 1 | Design and characterization of IFP PCA. (a) Modified secondary structure of the chromophore-binding domain of *D. radiodurans* (DrCBD) with the selected cut sites¹¹.

(b) Crystal structure displaying the location of the functional cut site. (c) Time course for association of biliverdin-HCl to overexpressed zipper IFP PCA in a lysate of yeast cells (error bars, s.d.; $n = 3$ independent experiments). (d) Fluorescence spectra of the indicated proteins at equal concentrations. a.u., arbitrary units. (e) Cumulative distribution function displaying forward light scatter versus fluorescence. RFU, relative fluorescence units. (f) IFP PCA fluorescence signal for the indicated protein complexes expressed in yeast. A homodimerizing zipper and the non-interacting Skn7t and Ypd1* (NC) are positive and negative controls, respectively (error bars, s.d.; $n = 3$ independent experiments). (g) Test of spontaneous IFP PCA signal between non-interacting proteins (Skn7t and Ypd1*; NC) expressed at various levels in yeast cells using the indicated promoters (error bars, s.d.; $n = 9$ independent experiments). Cells that were transformed with plasmids encoding Skn7t-IFP-F[1] and Ypd1*-IFP-F[2] were then transformed with Ssk1t-IFP-F[1]. The interaction between Ssk1t and Ypd1* is detected as IFP PCA activity (NC/Ssk1t-IFP-F[1]). Ssk1t-IFP-F[1] and Ypd1*-IFP-F[2] serve as the positive control (error bars indicate s.e.m., $n = 9$ fields of view in one experiment). (h) IFP PCA signal for interaction between Ras and mutant versions of Raf. *In vitro* dissociation constants are listed above each result¹⁴. N.D., not detected *in vitro* or by IFP PCA. The fluorescence measurement is an average from images of 10 cells representative of three independent experiments (error bars, s.d.; $n = 10$).

(Supplementary Table 5). All Ras-RBD mutant interactions were detectable with K_D values up to 14 μM , and the decreases in signal were inversely correlated with *in vitro* K_D values^{14,16} (Fig. 1h).

We tested for reversibility of the IFP PCA by examining whether fragments dissociate following proteolysis. We inserted tobacco etch virus (TEV)-protease sites into the full-length IFP1.4 at the cut site (residues 132–133) or into the fusion proteins F_{M1}-IFP-F[1] and F_{M1}-IFP-F[2] (Supplementary Figs. 1e,f and 2a,b). We performed TEV-protease digestion followed by immunoprecipitation (anti-hemagglutinin (anti-HA) antibody (bound)) and western blotting. In both cases, proteolysis resulted in complete unfolding and dissociation of the fragments.

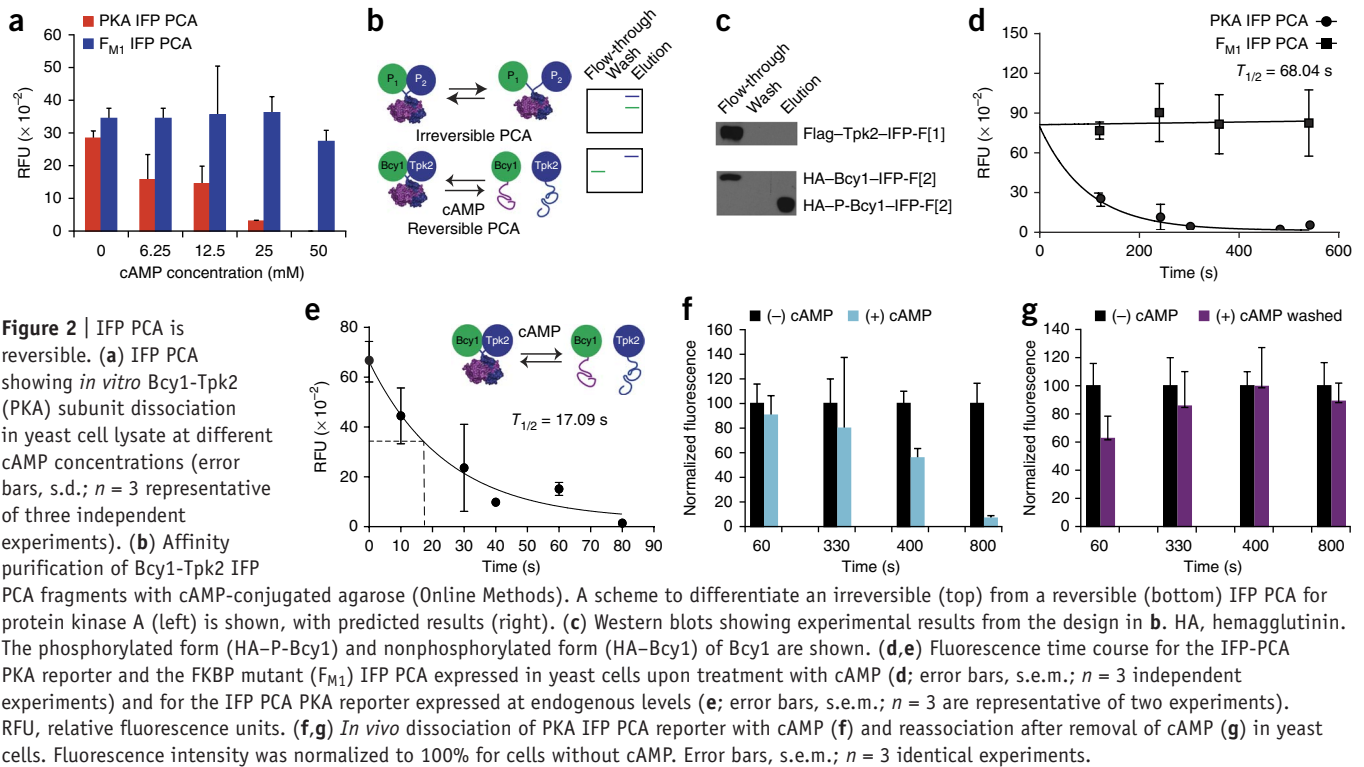
We next tested for reversibility for the cAMP-induced dissociation of the yeast PKA catalytic and regulatory subunits (Tpk2-Bcy1)¹⁷; this is an excellent test system because quantitative studies of its dissociation have been measured by different methods⁷. First, in lysate of cells expressing the Tpk2-Bcy1 reporter IFP PCA, we titrated cAMP levels and observed reduction of IFP PCA with addition of 50 mM cAMP (Fig. 2a). The *in vivo* Tpk2-Bcy1 interaction was also completely disrupted at 25 mM cAMP. Similar concentrations of cGMP had no effect (Supplementary Fig. 1d and Supplementary Table 3). Further, lysates from yeast cells expressing the Tpk2-Bcy1 PCA were applied to cAMP-conjugated



resin. Binding of Bcy1 to cAMP induces dissociation of the Tpk2-Bcy1 complex. If the IFP PCA remains folded, then we should detect both Bcy1 and Tpk2 resin bound, but if the IFP unfolds, only Bcy1 will be resin bound. Western blot analysis of purified fractions showed only Bcy1 bound to resin, and Tpk2 was detected in the flow-through (Fig. 2b,c and Supplementary Fig. 2c). Thus, the IFP fragments unfold upon dissociation of Tpk2-Bcy1.

Finally, we determined dissociation rates of Tpk2-Bcy1 *in vivo* after addition of cAMP (Fig. 2d,e). We observed complete dissociation of complexes, with distinct half-maximal time values ($T_{1/2}$) if the PCA reporter was overexpressed ($T_{1/2} = 68$ s) or endogenously expressed ($T_{1/2} = 17$ s). These results illustrate that the IFP PCA is readily reversible *in vivo* and with rates consistent with those reported by other methods; the results also demonstrate the importance of expressing reporters at endogenous levels to determine accurate dynamic parameters. The reassociation of Tpk2-Bcy1 after removal of cAMP was readily detectable (Fig. 2f,g).

We constructed a mammalian PKA IFP PCA reporter using catalytic subunit α (Cat) and regulatory subunit type II β (Reg) to detect signaling of the β_2 -adrenergic receptor (β_2 -AR) in U2OS cells^{17,18} (Supplementary Tables 1 and 2). Signal was modulated



by the β_2 -AR agonist isoproterenol with a half-maximal effective concentration $EC_{50} = 1.18$ nM (Fig. 3a,b), and $T_{1/2} = 46.7$ s (at 10 μ M isoproterenol), comparable to values observed in other studies; and the β_2 -AR-specific antagonist, alprenolol, prevented dissociation of PKA⁷ (Fig. 3b,c). Reduction of the PKA IFP PCA reporter signal was not due to bleaching (Supplementary Fig. 1c and Supplementary Table 3).

To demonstrate application of IFP PCA to spatiotemporal dynamics, we chose the yeast pheromone-induced relocalization of Fus3-Ste5 complex to mating projections (shmoo). Spatiotemporal analysis of Fus3-Ste5 has been previously performed, and there are only 1–10 Fus3-Ste5 complexes at the shmoo; therefore, this experiment tests the limits of sensitivity of the IFP PCA¹⁹.

We integrated IFP fragments F[1] and F[2] into the loci of *FUS3* and *STE5*, respectively, 3' to their coding sequences, in *MATA* cells (Supplementary Table 6) and performed epifluorescence microscopy for cells that were either treated with the pheromone α -factor (10 μ M) or untreated (Online Methods). Treatment with α -factor resulted in translocation of Fus3-Ste5 from a diffuse peripheral cytosolic distribution to multiple foci at the surface of some cells, resolving to single foci at the shmoo tip by 3.5 h (Fig. 4a,b and Supplementary Fig. 3).

Finally, to demonstrate detection of both induction and dissociation of a protein complex, we used the SHC1-GRB2 interaction, whose temporal modulation by epidermal growth factor (EGF) receptor has been reported²⁰. We created SHC1-GRB2 PCA

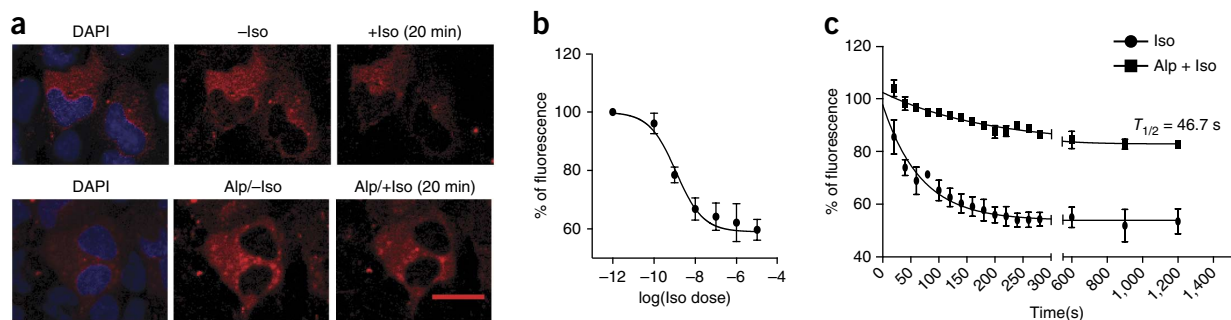
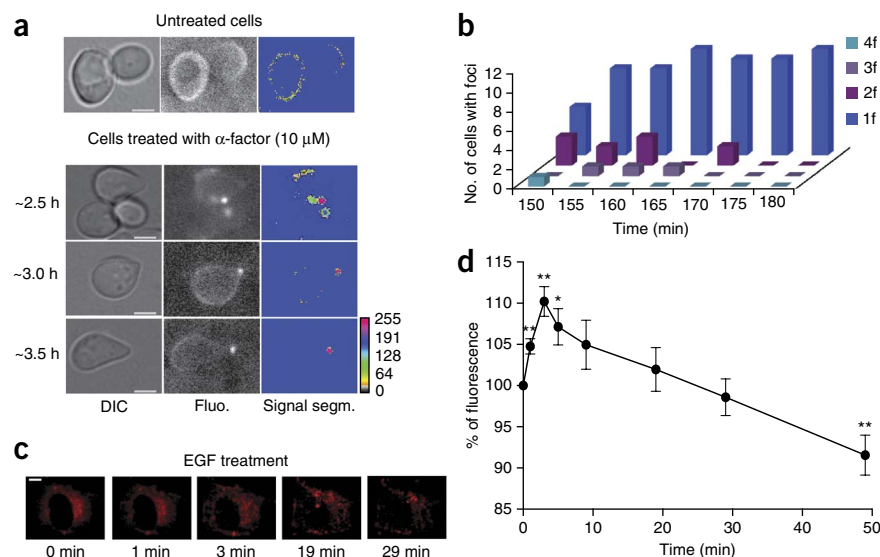


Figure 3 | IFP PCA reversibility in mammalian cells. (a) U2OS cells stably expressing the IFP PCA reporter for PKA (regulatory PKA subunit RII β IFP-F[2] and catalytic subunit α Cat α IFP-F[1]) before and after the addition of isoproterenol (Iso), an agonist of the β_2 -adrenergic receptor (β_2 -AR), and alprenolol (Alp), a β_2 -AR antagonist that prevents Iso-induced dissociation of the RII β :Cat complexes. (b) Dose-response of the PKA IFP PCA reporter in U2OS cells treated with Iso at the following concentrations: 0.1 nM, 1 nM, 10 nM, 100 nM, 1 μ M and 10 μ M. Fluorescence signal of the cells was quantified for each Iso dose and normalized to the signal without Iso. On average, 17 cells were analyzed per Iso dose; error bars, s.e.m.; $n = 3$ fields of view. (c) Time course of the PKA IFP PCA reporter in U2OS cells treated with Iso and Alp. Stacks of fluorescence images of the IFP PCA were acquired at a magnification of 20 \times , and the fluorescence intensity was normalized to 100% at t_0 and represented here by percentage of fluorescence. ~ 300 cells were analyzed for Iso treatment and ~ 200 cells for Iso + Alp treatment. Error bars, s.e.m.; $n = 3$ fields of view for Iso, and $n = 2$ fields of view for Alp + Iso. Observations are representative of 3 independent experiments. Scale bar, 25 μ m.

Figure 4 | Spatiotemporal localization of protein complexes in living eukaryotic cells. **(a)** Differential interference contrast (DIC), segmented (Signal segm.) and unsegmented (Fluo.) fluorescence images of yeast expressing IFP PCA–reported Fus3–Ste5 complexes, before (top) and after (bottom) treatment with pheromone (α -factor). Scale bars, 4 μm . **(b)** Distribution of IFP PCA–reported Fus3–Ste5 complexes that are in foci. The number of cells with foci (f) (1, 2, 3 or 4 foci) in pheromone-responding cells was examined for up to 3 h in 30-min intervals. Pheromone was added at t_0 , and the first foci were observed in most cells at about 150 min; data for the 150- to 180-min time window in 5-min intervals are shown. **(c)** IFP PCA signal for the SHC1–GRB2 complex in response to EGF, in HeLa cells. Scale bar, 10 μm . **(d)** Fluorescence intensity as in **c** was quantified and normalized to 100% at t_0 . Error bars, s.e.m.; $n = 20$ HeLa cells; observations are representative of 3 independent experiments. * $P < 0.05$, ** $P < 0.005$ relative to t_0 (Student's t -test).



reporter plasmids (**Supplementary Tables 1 and 2**) and transformed them into HeLa cells (Online Methods). As also reported by Zheng *et al.*²⁰, we observed that the SHC1–GRB2 interaction reached a maximum at ~ 3 min after EGF stimulation, followed by recovery with $T_{1/2}$ of ~ 30 min, and that the distribution of complexes changed from being diffuse at the cell surface to being localized in multiple foci. These foci were likely endosomes because the IFP PCA signal colocalized with LysoTracker-stained particles (**Fig. 4c,d**, **Supplementary Video 1** and **Supplementary Fig. 4f**).

The IFP PCA is a simple technique that can be used to detect spatiotemporal dynamics of protein complexes in living cells at low abundances of 10–100 copies. Limitations of the IFP PCA are its low quantum yield, low brightness and the requirement for exogenously added biliverdin, which is, however, inexpensive, available and readily enters cells *in vivo*¹⁰. The recently reported iSplit PCA based on the iRFP is ten times brighter than the IFP1.4 PCA reported here and does not require exogenous biliverdin, but the irreversibility of iSplit, as with other fluorescent protein PCAs, prevents its application to quantitative studies of PPI spatiotemporal dynamics¹². The steric requirements for refolding PCA reporters from fragments mean that they can be used as molecular rulers at nanometer resolution, higher than that of optical super-resolution techniques. Indeed, we have defined the topological organization of an entire proteome at 8-nm resolution using another PCA⁸. The IFP PCA could also be a powerful tool for studying PPI on a large scale for any organism, including humans¹¹. For all applications, improvements of quantum yield by directed evolution would lead to an even more powerful tool. Finally, the lack of apparent cytotoxicity, low light scattering and absorption in deep tissues, and thus low attenuation of infrared light, makes the IFP PCA a versatile reporter system for imaging biochemical processes in living organisms¹¹.

METHODS

Methods and any associated references are available in the [online version of the paper](#).

Accession codes. Addgene: 52893, 52895, 52896, 52897, 52898, 52899, 52900, 52901, 52902, 52903, 52905, 52906, 52907.

Note: Any Supplementary Information and Source Data files are available in the [online version of the paper](#).

ACKNOWLEDGMENTS

We thank R.Y. Tsieng (University of California) for providing the pBADb2e IFP1.4–H01 plasmid, S. Kalynych from the M. Cygler laboratory (University of Saskatchewan) for providing us with the bacterial plasmid p15A-Kan and G. Ferbeyre (Université de Montréal) for providing the pLpC retroviral vector. We also thank C. Mazurek, P.H. Ear, M. Malleshaiah, V. Messier, V. Bourdeau, E. Querido, D. Gagné and M. Vasseur for support and discussions. The authors acknowledge support from Canadian Institutes of Health Research grants MOP-GMX-152556 and MOP-GMX-231013 and Natural Sciences and Engineering Research Council of Canada grant 194582 (to SWM).

AUTHOR CONTRIBUTIONS

E.T. designed the experiments, engineered IFP PCA fragments, generated constructs, developed and performed assays in *E. coli* and *S. cerevisiae*, analyzed the results and wrote the manuscript. D.S. designed experiments with mammalian cells (U2OS and HeLa), generated constructs and stable cell lines, analyzed the results and wrote the manuscript. S.W.M. designed the experiments, supervised the project, analyzed the results and wrote the manuscript.

COMPETING FINANCIAL INTERESTS

The authors declare no competing financial interests.

Reprints and permissions information is available online at <http://www.nature.com/reprints/index.html>.

- Ghosh, I., Hamilton, A.D. & Regan, L. *J. Am. Chem. Soc.* **122**, 5658–5659 (2000).
- MacDonald, M.L. *et al. Nat. Chem. Biol.* **2**, 329–337 (2006).
- Hu, C.D., Chinenov, Y. & Kerppola, T.K. *Mol. Cell* **9**, 789–798 (2002).
- Johnsson, N. & Varshavsky, A. *Proc. Natl. Acad. Sci. USA* **91**, 10340–10344 (1994).
- Michnick, S.W., Ear, P.H., Manderson, E.N., Remy, I. & Stefan, E. *Nat. Rev. Drug Discov.* **6**, 569–582 (2007).
- Remy, I. & Michnick, S.W. *Nat. Methods* **3**, 977–979 (2006).
- Stefan, E. *et al. Proc. Natl. Acad. Sci. USA* **104**, 16916–16921 (2007).
- Tarassov, K. *et al. Science* **320**, 1465–1470 (2008).
- Michnick, S.W., Remy, I., Campbell-Valois, F.X., Vallée-Bélisle, A. & Pelletier, J.N. *Methods Enzymol.* **328**, 208–230 (2000).
- Shu, X. *et al. Science* **324**, 804–807 (2009).
- Wagner, J.R., Brunzelle, J.S., Forest, K.T. & Vierstra, R.D. *Nature* **438**, 325–331 (2005).
- Filonov, G.S. & Verkhusha, V.V. *Chem. Biol.* **20**, 1078–1086 (2013).
- Bornschrögl, T. *et al. Biophys. J.* **96**, 1508–1514 (2009).
- Ear, P.H. & Michnick, S.W. *Nat. Methods* **6**, 813–816 (2009).
- Mumberg, D., Müller, R. & Funk, M. *Gene* **156**, 119–122 (1995).
- Block, C., Janknecht, R., Herrmann, C., Nassar, N. & Wittinghofer, A. *Nat. Struct. Biol.* **3**, 244–251 (1996).
- Taylor, S.S. *et al. Biochim. Biophys. Acta* **1697**, 259–269 (2004).
- Pierce, K.L., Premont, R.T. & Lefkowitz, R.J. *Nat. Rev. Mol. Cell Biol.* **3**, 639–650 (2002).
- Malleshaiah, M.K., Shahrezaei, V., Swain, P.S. & Michnick, S.W. *Nature* **465**, 101–105 (2010).
- Zheng, Y. *et al. Nature* **499**, 166–171 (2013).

ONLINE METHODS

Selection of PCA fragment dissection sites. Dissection sites were chosen in unstructured regions of IFP1.4 DrCBD, PDB ID: 1ZTU (ref. 11), except for R222, located on the ninth β -strand of the GAF domain. Because the mechanism of chromophore assembly of the apo protein was reported to be post-translational, seven cut sites were chosen around the GAF domain (F170, R192, R218, V252, T256, V269, T293). Two out of the last five cut sites were chosen at the interface between both GAF and PAS domains (W132, T242), and three other sites were chosen in the PAS domain (H38, P58, L62). With the exception of T242, all sites were chosen to be as far from the figure-eight knot in three-dimensional space as possible.

Construction of plasmids and cassettes. Bacterial constructs. To test the ability of pairs of IFP1.4 fragments to produce a working PCA at each cut site, sequence coding for GCN4 leucine zipper with a ten-amino-acid flexible peptide linker (Gly-Gly-Gly-Gly-Ser)₂ was amplified by PCR from pCDNA3.1-Zip-mDHFR-F[1,2] (ref. 8) as template using the Phusion polymerase and positioned at the 5' end of the PCA fragments. Next, the above PCR-amplified zipper and linker product was subcloned into the restriction sites BamHI and SacI of the plasmid pBAD-6xhis-IFP1.4-HO-Amp (ref. 10) at the 5' end of IFP1.4, resulting in the construct pBAD-6xhis-zipper-IFP1.4-HO-Amp. Thirteen N-terminal fragments (IFP-F[1]_X) were amplified by PCR together with zipper and linker from the construct pBAD-6xhis-zipper-IFP1.4-HO-Amp and subcloned into the EcoRI and XbaI restriction sites of pBAD-p15A-Kan (kindly provided by S. Kalynych²¹), resulting in the constructs pBAD-p15A-6xhis-zipper-IFP-F[1]_X-Kan. The 13 corresponding C-terminal fragments (IFP-F[2]_Y) were amplified by PCR and subcloned using classical cloning procedures into the SacI and XbaI restriction sites replacing the fragment M3F2 (with no intrinsic fluorescence) in the construct pBAD-6xhis-zipper-M3F2-HO-Amp, resulting in pBAD-6xhis-zipper-IFP-F[2]_Y-HO-Amp. All plasmid DNA constructs were amplified in *E. coli* DH5 α and verified by sequencing.

Yeast constructs. IFP PCA fragments were PCR amplified from the bacterial constructs above using primers including the sequences to restriction sites (XhoI and XbaI). The resulting Zipper-Linker-IFP-F[2] fragments were subcloned into XbaI and XhoI restriction sites of p413-GAL 1 (Addgene), and Zipper-Linker-IFP-F[1] fragments were introduced into XbaI and XhoI sites of p416-GAL 1 (Addgene). Plasmids p413-GAL 1 and p416-GAL 1 contained, respectively, the selection markers histidine (*HIS3*) and Uracil (*URA3*) that are used to select for transformation of *MATa* cells grown on medium containing auxotrophic amino acids. All constructs were amplified in *E. coli* DH5 α and validated by sequencing. To demonstrate the functionality, specificity and reversibility of the IFP-PCA, we generated further constructs where the zipper sequence was replaced by genes coding for interacting proteins (Ssk1t, Skn7t, Ypd1 (W80A), Bcy1, Tpk2, F_{M1}, Ras, Raf-RBD-wild type, RBD mutants (K84A, N64A, Q66A, T68A, R59A, R89L)) in XbaI and ClaI restriction sites of the constructs p416-Gal1-Zip-IFP-F[1]₁₋₁₃₂ or IFP-F[2]₁₃₃₋₃₂₁. Owing to the presence of internal ClaI restriction sites in the protein Ypd1 (W80A), a fusion product of that gene with linker and IFP-F[2] was generated by SOE-PCR (splicing by overlap extension). The constructs Ssk1t-IFP-F[1], Skn7t-IFP-F[1]

and Ypd1-IFP-F[2] were expressed under different promoters: *GAL*, *TEF*, *GPD* and *ADH*. All subcloning was carried out using standard cloning techniques²².

Construction of yeast homologous recombination cassettes. To visualize and localize Ste5-Fus3 complexes in pheromone-treated *MATa* cells, we endogenously tagged the genes respectively with IFP-F[1]₁₋₁₃₂ and F[2]₁₃₃₋₃₂₁ (henceforth referred to as IFP-F[1] and IFP-F[2]). IFP PCA fragments were PCR amplified from yeast expression vectors that harbor these sequences and subcloned into pAG25-linker-DHFR F[1,2] and pAG32-linker-DHFR F[3] plasmids between HindIII and XbaI restriction sites. This resulted in the replacement of the linker-DHFR F[1,2] fragment with linker-IFP-F[1], creating the pAG25-linker IFP-F[1]₁₋₁₃₂ construct; likewise, the linker-DHFR F[3] was replaced with linker-IFP-F[1] F[1] to yield pAG32-linker IFP-F[2]. Furthermore, plasmids pAG25-IFP-F[1] and pAG32-IFP-F[2] also code for unique antibiotic resistance cassettes, which are located 5' to an *ADH* terminator sequence (*ADHter*)²³. Thus the final IFP-F[1] template (pAG25-IFP-F[1]) consists of pAG25-linker-IFP-F[1]-*ADHter* followed by the *TEF* gene promoter and the nourseothricin *N*-acetyltransferase (*NAT1*) gene that confers resistance to Clonate and, finally, a *TEF* terminator. The final IFP-F[2] template (pAG32-IFP-F[2]) consists of pAG32-linker-IFP-F[2]-*ADHter* followed by the *TEF* promoter, hygromycin-B phosphotransferase gene (*HPH*) that confers resistance to hygromycin-B and, finally, the *TEF* terminator. The above templates were used to PCR-amplify homologous recombination cassettes to introduce IFP PCA fragments 3' to the open reading frames (ORF) of the genes studied here (*STE5*, *FUS3*, *BCY1* and *TPK2*). *STE5* and *BCY1* were fused to IFP-F[2], whereas *FUS3* and *TPK2* were fused to IFP-F[1]. Therefore, the IFP fragments were integrated 3' to the ORFs in the *Saccharomyces cerevisiae* genome by homologous recombination to ensure endogenous levels of expression from their natural loci. Oligonucleotide design for PCR amplification of the IFP PCA cassettes, their synthesis, PCR amplification and homologous recombination methods are identical to those described previously¹⁹.

Construction of plasmids for expression in mammalian cells. IFP-F[1] and IFP-F[2] were PCR amplified along with the ten-amino-acid linker 5' to the IFP-F[1] and IFP-F[2] using the p15A-Histag-Zip-IFP-F[1] and pBAD-Histag-Zip-IFP-F[2] HO-1 as templates and further subcloned into pLpCMCS binary vector (kindly provided by G. Ferbeyre) within the ClaI and EcoRI restriction sites to create the pLpC IFP-F[1] and pLpC IFP-F[2], respectively. The catalytic (mouse, type α , Cat) subunit of the PKA was PCR amplified using pCDNA3.1Cat-Rluc F[2] (ref. 7) as template and further subcloned into pLpC IFP-F[1] plasmid within the PacI and ClaI restriction sites to generate pLpCCat-IFP-F[1]. The IFP-F[2] fragment was PCR amplified from pBAD-Histag-Zip-IFP-F[2]-HO-1 and subcloned into pCDNA3.1RegRluc-F[1] (ref. 7) that contains the regulatory subunit (rat, type II β , Reg) within BspEI and XbaI, resulting in the fusion between Reg and IFP-F[2] with the ten-amino-acid linker between the two gene fragments, pCDNA3.1Reg-IFP-F[2]. To construct pLpCReg-IFP-F[2] plasmid, we PCR-amplified the Reg-IFP-F[2] from the pCDNA3.1Reg-IFP-F[2], followed by subcloning into pLpCMCS binary vector between the PacI and EcoRI restriction sites. Finally, the construction of pLpCReg-IFP-F[2] + Venus and pLpCCat-IFP-F[1] + mPlum binary vectors were created by inserting the

PCR amplified Venus and mPlum fragments between the PmeI and SalI restriction sites found in the multiple cloning sites following the IRES sequence. Similarly, to test the interaction between SHC1 and GRB2, the *SHC1* and *GRB2* cDNA was PCR amplified from Gateway cloning vectors and subcloned into PacI and ClaI restriction sites within the pLpC vectors harboring the IFP-F[1] + mPlum and pLpC IFP-F[2] + Venus cassettes, thereby creating the pLpCSHC1-IFP-F[1] + mPlum and pLpCGRB2-IFP-F[2] + Venus. All plasmid DNA constructs were verified by sequencing.

Accession codes. The Addgene IDs are followed by the corresponding identification of the plasmid below. ID 52893, p413GAL1-Zipp.-L-IFP-F[2] (yeast); 52895, p416GAL1-Zipp.-L-IFP-F[1] (yeast); 52896, p416GAL1-Skn7t-L-IFP-F[1] (yeast); 52897, p416GAL1-Ssk1t-L-IFP-F[1] (yeast); 52898, p413GAL1-Ypd*1-L-IFP-F[2] (yeast); 52899, pAG25-L-IFP-F[1] (clon 3); 52900, pAG32-L-IFP-F[2] (clon 3); 52901, pLpC-L-IFP-F[1] (mammalian); 52902, pLpC-L-IFP-F[2] (mammalian); 52903, pLpC-Reg-L-IFP-F[2]+Venus (mammalian); 52905, pLpC-Cat-L-IFP-F[1]+Plum (mammalian); 52906, pLpC-Zipp.-L-IFP-F[2]+Venus (mammalian); 52907, pLpC-Zipp.-L-IFP-F[1]+Plum (mammalian).

Biophysical analysis of IFP-PCA. *Protein purification.* In order to express and purify the functional combinations of C- and N- fragments, the protocol described below (see the “*In vivo* screening” section below) for protein expression in Rosetta cells was adapted to a larger volume culture (1 liter). Cells were harvested through centrifugation at 3,185g for 20 min (Eppendorf Centrifuge 5810R) and were frozen at -80°C . Then the cell pellet was thawed on ice and mixed with lysis buffer before sonication (Branson Sonifier 450, Ultrasonics Corporation) for 2 min in steps of 30 impulses. The purification of His₆-tagged protein was performed according to the QIAexpressionist manual (Qiagen) under nondenaturing conditions. Briefly, the cell pellet was resuspended in lysis buffer adjusted to pH 8 (50 mM NaH₂PO₄, 300 mM NaCl, 10 mM imidazole, 2 mM β -mercaptoethanol). The lysate was clarified for 30 min at 12,000g (Sorvall RC-5B, DuPont Instruments) and incubated with Ni²⁺-NTA slurry at 4 $^{\circ}\text{C}$ for 3 h. The lysate-and-slurry mix was transferred to a column, and nonspecific binders were eluted with wash buffer (50 mM NaH₂PO₄, 300 mM NaCl, 20 mM imidazole, pH 8). The elution buffer (50 mM NaH₂PO₄, 300 mM NaCl, 250 mM imidazole, pH 8) was used to dissociate the protein from the resin. The purified protein was dialyzed for 2 h at 4 $^{\circ}\text{C}$ against 1 \times phosphate buffered saline (PBS) diluted from 10 \times PBS stock (1.4 M NaCl, 27 mM KCl, 100 mM Na₂HPO₄, 18 mM KH₂PO₄, pH 7.4) followed by another dialysis step in a new flask of 1 \times PBS overnight at 4 $^{\circ}\text{C}$. We added 4 $\mu\text{g ml}^{-1}$ biliverdin-HCl in order to saturate the protein and incubated the mix at 4 $^{\circ}\text{C}$ for 20 min. The samples were either directly analyzed by spectroscopy in quartz cuvettes (Photometer cell VWR # 414004-068) (Cary Eclipse Spectrofluorimeter, Varian) or distributed into aliquots and kept at -80°C for later analysis.

Quantum yield and extinction coefficient determination. Fluorescence measurements of the purified zipper/zipper-IFP PCA and IFP1.4 full length were taken on the SpectraMax Gemini-XS (Molecular Devices). This system is a dual-monochromator microplate fluorometer system that enables wavelength scanning from 250 nm to 850 nm in increments as small as 1 nm. Emission

scans were performed on samples dispensed in Corning Costar special optics plates (96-well flat-bottom, black with extra-thin clear bottom). Emission scans were conducted with excitation fixed at 640 nm, and the absorption was measured between 320 nm and 750 nm in increments of 5 nm. Four different concentrations of IFP1.4 full length and Zipper IFP PCA were measured in triplicate. The Gemini-XS instrument was autocalibrated for each wavelength required for this experiment in order to have high accuracy in measurements. A comparative method was employed to determine the fluorescence quantum yield (ϕ_F) of the IFP PCA, using IFP1.4 full length with known ϕ_F of 0.07 as a reference^{10,24}. The ϕ_F for IFP PCA was calculated by plotting the integrated fluorescence intensity against the absorbance from the solutions with known concentrations. The ϕ_F was obtained from the ratio of the slopes resulting from the linear fits of the plots generated from IFP PCA and IFP1.4, respectively. IFP PCA extinction coefficient (ϵ) was determined on the basis of the assumption that absorbance at 388 nm was due to bound biliverdin and that ϵ_{388} of the IFP-PCA is equal to that of free biliverdin-HCl, 39,900 M⁻¹ cm⁻¹ (refs. 10,25) using the Beer-Lambert law ($A = \epsilon cl$)²⁴.

Maturation rate. Maturation time for the IFP PCA was determined with lysate of yeast cells expressing overnight the cassettes zip-(Gly₄Ser)₂ IFP-F[1] and zip-(Gly₄Ser)₂ IFP-F[2] expressed off a GAL promoter in plasmids p416 and p413, respectively. The cell lysate was prepared as described in the subsection “Protein expression and screening in yeast cells” below (and “IFP PCA reversibility *in vitro*”). Samples of clarified cell lysate were then incubated with saturating amounts of biliverdin-HCl (133 $\mu\text{g ml}^{-1}$) on ice for 63 min, 48 min, 33 min, 18 min and 5 min, and fluorescence signal measurement was carried out with the spectrophotometer (SpectraMax Gemini-XS).

***In vivo* screening for functional PCA combinations.** *IFP PCA screening in bacteria.* Pairs of plasmids harboring coding sequences for the different N- and C-fragment pairs of IFP1.4 fused to the sequence of the homodimerizing leucine zipper and a ten-amino-acid flexible linker peptide were successively transformed into the *E. coli* expression strain Rosetta (DE3). For example, first the construct pBAD-6xhis-zipper-IFP-F[2]-HO-Amp was used to transform electrocompetent Rosetta (DE3) cells, which were incubated overnight on LB broth with agar (LB) containing selection marker (100 $\mu\text{g ml}^{-1}$ ampicillin with 25 $\mu\text{g ml}^{-1}$ chloramphenicol) at 37 $^{\circ}\text{C}$. The next day, one colony was isolated to prepare a preculture for making new electrocompetent cells²². The latter were transformed by introduction of the second construct (pBAD-p15A-6xhis-IFP-F[1]) and incubated on LB with appropriate selection markers (100 $\mu\text{g ml}^{-1}$ ampicillin, 50 $\mu\text{g ml}^{-1}$ kanamycin and 25 $\mu\text{g ml}^{-1}$ chloramphenicol). Single colonies were isolated from the agar plates to prepare overnight cultures. These were then used to inoculate 18 ml of fresh LB medium with appropriate antibiotics. At OD₆₀₀ of 0.6, the culture was distributed into two different test tubes. One test tube was filled with 3 ml of LB containing 8% arabinose to induce protein expression, whereas the other test tube was filled with 3 ml LB, and 8% glucose was added to inhibit gene expression. Prior to measurements, the bacterial cultures were incubated at 37 $^{\circ}\text{C}$ for 2 h and then a further 4 h following addition of 4 $\mu\text{g ml}^{-1}$ biliverdin-HCl (Frontier scientific #B14022). The cultures were centrifuged at 500g for 10 min, the supernatant was discarded and 320 μl of

1× PBS was added to the pellet and cells were resuspended. The samples (100 µl) were analyzed in black-walled microtiter plates with clear bottoms (Corning, #3614) using the spectrofluorometer SpectraMax Gemini-XS with the following settings: excitation wavelength = 640 nm, emission = 708 nm, 30 s of shaking followed by signal integration over 30 reads. The experiments were either repeated independently (biological replicates) or performed in triplicate using the same biological material (technical replicates). Expression levels of various IFP PCA combinations were quantified as change in relative fluorescence units between the induced and non-induced cells.

Screening for high levels of IFP PCA expression in bacteria. We randomly picked 384 clones expressing IFP Zip-F[1]1-132 and Zip-IFP F[2]133-321, regrew the cultures in 100 µl LB with antibiotics (100 µg ml⁻¹ ampicillin, 50 µg ml⁻¹ kanamycin and 25 µg ml⁻¹ chloramphenicol) on a microtiter plate (Corning, #3707) and selected clones producing the highest fluorescence signal. After 4–6 h of incubation at 37 °C, the saturated cultures were mixed with glycerol at a final concentration of 20% and kept at –80 °C as master plates. For dual expression of PCA fragments, bacterial cells from glycerol stock were transferred to a new microtiter plate containing 75 µl fresh LB with antibiotics and grown to OD₆₀₀ of 0.7 after 4 h of incubation at 37 °C. Then induction of protein expression followed with 25 µl LB containing antibiotics and 0.8% L-arabinose grown overnight. After overnight incubation at 28 °C/200 r.p.m./65% humidity (16–18 h), the bacterial cultures were diluted to OD₆₀₀ of 0.8 before analysis using a flow cytometer for high-throughput acquisition (LSR II Flow Cytometer, Becton Dickinson). Flow cytometry data were collected for 10,000 cells excited with a 633-nm laser with signal detection of maximal emission between 680 nm and 710 nm (APC-Cy5.5 detector).

Protein expression and screening in yeast cells. Before we started the functional assays in yeast, another screening of the different IFP PCA fragments was performed in yeast. Five cut-site combinations were selected on the basis of the first screen conducted in Rosetta cells. Chemically competent *MATa* cells (strain BY4741) were transformed with corresponding yeast constructs and plated onto synthetic minimal medium with ammonium sulfate (0.67% yeast nitrogen base, 2% Bacto agar, 2% glucose and 5% amino acids cocktail) and allowed to grow at 30 °C for 3 d. Colonies were isolated to inoculate synthetic liquid medium using the appropriate selection marker and 2% raffinose to prepare saturated precultures. The next day, fresh cultures with the same medium composition were inoculated at OD₆₀₀ of 0.2. After 4 h of incubation, the culture was divided into two equal volumes (A and B) and transferred to sterile tubes. To culture A, 2% galactose was added to induce protein expression, whereas culture B was enriched with 2% glucose as a negative control. In order to maintain the same growth rate among populations, 2% glucose was used instead of raffinose. Cells were induced for 2 h before addition of biliverdin-HCl (Frontier scientific #B14022) to a final concentration of 4 µg ml⁻¹, and cells were further incubated for 3–4 h at 30 °C/600 r.p.m. Flow cytometry was carried out with the same settings described above for bacterial cells. The optical density of cultures was set equally at 10⁷ cells ml⁻¹ before collecting the pellet from 40 ml for 5 min at 800g. The pellet was resuspended in 350 µl of 1× low-fluorescence medium (LFM)¹⁹ for triplicate analysis with a spectrofluorometer as described above for bacteria.

Demonstration of IFP PCA reversibility. *IFP PCA reversibility in yeast.* Yeast PKA catalytic subunit Tpk2 was tagged at its C terminus with IFP-F[1] and at its N terminus with a Flag tag, whereas Bcy1 was fused to the C terminus of IFP-F[2] as described above. Overexpression of the fusion proteins in *MATa* was carried out as described in the previous section. Briefly, the culture (20 ml of 10⁶ cells ml⁻¹) was centrifuged at 800g for 5 min to collect the pellet, which was carefully resuspended in 500 µl of LFM with biliverdin-HCl (10 µg ml⁻¹). Samples were analyzed in triplicate, with addition of 25 mM Na-cAMP (Sigma #A6885) or 25 mM of Na-cGMP (Sigma #G6129). After 2 min of incubation at room temperature, the fluorescence signal was measured with a spectrofluorometer, as described above, in each sample and compared to a control sample of sterile deionized water.

To determine the rate of dissociation of the yeast PKA subunits, either endogenously expressed from their natural loci as fusion proteins with IFP PCA fragments or overexpressed from plasmids under the *GAL* promoter, we measured the fluorescence over time using the spectrofluorometer (SpectraMax Gemini-XS). The measurement was carried out before addition of cAMP and then 2 min, 4 min, 5 min and 9 min after cAMP addition to cells overexpressing the fusion proteins or directly measured by integration of signal over 20 s following cAMP (6.25 mM) addition to cells expressing the fusion proteins endogenously because of low levels of expression. *MATa* cells overexpressing dimerizing F_{M1} (FKBP mutant) protein tagged with IFP PCA fragments were used as a control. A further experiment with overexpressed yeast PKA subunits as fusion proteins to IFP-PCA fragments was performed to evaluate the reconstitution of the PKA signal after washing off the cAMP (10 mM) added to the cells. After addition of cAMP, the suspension was carefully mixed and incubated at room temperature for 10 min. Then cells were washed with 1× LFM at 800g for 5 min and resuspended with 400 µl of LFM with biliverdin-HCl (10 µg ml⁻¹). Fluorescence resulting from the reassociation of IFP-PCA fragments was measured on 110 µl of the cell suspension at 60 s, 330 s, 400 s and 800 s. A suspension with same amount of untreated cells was used as a control.

IFP PCA reversibility in vitro. Overexpressed Tpk2-IFP-F[1] and Bcy1-IFP-F[2] fusion proteins were isolated from *BCY1Δ* *MATa* cells with the yeast protein extract buffer following procedures described elsewhere¹⁹. The cell lysate was used to quantify dissociation of yeast PKA subunits by Na₂-cAMP at various concentrations (6.25 mM, 12.5 mM, 25 mM and 50 mM) and allowed to incubate on ice for 2 min before measurement. As a negative control, the same Na₂-cAMP concentrations were used with F_{M1} (mutated form of FK506 binding protein (FKBP)) dimerizing proteins tagged with the IFP PCA fragments. To determine the rate of dissociation of the PCA fragments, a calibration curve was obtained through plotting relative fluorescence units against time, compared to serial dilutions of Alexa Fluor 680 (Invitrogen #A20008) measured by the spectrofluorometer with excitation at 640 nm and emission at 708 nm.

cAMP-agarose affinity purification for IFP PCA reversibility immunoassay. Clarified yeast cell lysate was incubated at 4 °C under agitation with cAMP- agarose (Sigma #A0144-5ML) in equilibration buffer (50 mM MOPS, pH 7, 50 mM NaCl, 1 mM DTT) modified from a method described elsewhere²⁶. The lysate-resin mix was transferred to a column and flow-through was collected by gravity flow. The column was washed twice with

the equilibration buffer, and resin-bound protein was eluted by adding 100 μl of elution buffer (20 mM MES, pH 5.8, 50 mM NaCl, 25 mM cAMP) and incubated at 4 °C for 30 min. Total protein of the flow-through fraction was precipitated using a saturated 75% ammonium sulfate solution to reach an end concentration of 25%.

Immunoprecipitation of HA-IFP-F[1]. Yeast cell pellet lysate was prepared using a protease-free yeast extraction buffer. The clarified lysate (300 μl) was mixed to 20 \times TEV buffer, 0.1 M DTT and 1–2 units μl^{-1} AcTEV protease (Life Technologies #12575-015) and incubated at 30 °C for 3 h. The AcTEV-reaction was then added to a 50- μl slurry of monoclonal anti-HA-conjugated agarose beads (Sigma-Aldrich #A2095) followed by mixing at 4 °C for 2 h. The beads were pelleted by centrifugation at 13,000g for 30 min, supernatant was removed and the pellet was washed once with 1 \times PBS. Proteins were eluted from the beads with a mixture of 70 μl of 1 \times PBS and 30 μl of 5 \times Laemmli sample buffer. The saved supernatant (70 μl) was mixed with 5 \times Laemmli sample buffer (30 μl) for further analysis.

All protein fractions were mixed with 5 \times SDS-PAGE buffer and boiled for 10 min before separation on a 12% SDS-PAGE gel. Standard methods were used for SDS-PAGE and western blots. Proteins were transferred to a PVDF membrane using the wet transfer method (Bio-Rad). After the transfer, the membrane was blocked with blocking solution (5% skim milk powder in 1 \times PBS, 0.05% Tween and 5% fetal calf serum (FCS)) for 2 h at room temperature, followed by 2 h incubation with chicken polyclonal anti-HA-HRP antibody (4 $\mu\text{g ml}^{-1}$, Abcam #ab1190) to detect the HA-Bcy1-IFP-F[2] and HA-IFP-F[2]. Whereas for detection of Flag-Tpk2-IFP-F[1] and Flag-IFP-F[1], anti-Flag antibody (8.6 $\mu\text{g ml}^{-1}$, Sigma #F3165-2mg) was used. After 90 min of incubation with the primary antibody, the membranes were washed three times for 10 min with 1 \times PBST (0.1% Tween) and three times with 1 \times PBS. After this, the membranes were incubated with secondary antibodies for 90 min with goat IgG anti-mouse-HRP (4.3 $\mu\text{g ml}^{-1}$, Cell Signaling Technology #7076S) to detect mouse anti-Flag antibodies. The membranes were then subjected to three times washing with 1 \times PBST followed by signal detection. For signal detection, electrochemiluminescent (ECL) reagent (PerkinElmer, # NEL 104 and NEL 105) was added to the blots for 60 s incubation at room temperature. Excess ECL reagent was removed, blots were then exposed to film (GE Healthcare #28906838), and the films were developed on a KODAK M35A X-OMAT processor.

Cell culture and imaging of IFP PCA in mammalian systems. U2OS and HeLa cells were grown and maintained in DMEM medium (Wisent) supplemented with 10% FBS. Stable cell lines of Reg-IFP-F[2]/Cat-IFP-F[1] in U2OS cell line were generated using retroviral gene transfer described elsewhere²⁷ using the pLpCReg-IFP-F[2]+venus and pLpCCat-IFP-F[1]+mplum plasmids. Briefly, cells were plated into 96-well plates (MGB101-1-2-LG, Matrical Bioscience) and incubated at 37 °C and in 5% CO₂, followed by addition of 40 μM of biliverdin-HCl for at least 3–4 h before imaging in DMEM minus phenol red. Cells were imaged using an InCell Analyzer 6000 (GE Healthcare) using a Cy5 filter (excitation, 642 nm; emission, 706.5/70 nm) with an integration time of 500 ms, and images were captured every 15 or 20 s. The cells were maintained at 37 °C throughout the experiment. Isoproterenol-HCl (Sigma) and alprenolol-hydrochloride (Sigma)

were added to cells, both at a concentration of 10 μM . All images were deconvoluted with MetaMorph software (version 7.5.3, MDS Analytical Technologies). Briefly, images that were acquired over an interval of 15- or 20-s time points were stacked, followed by initial processing to normalize background. Next, the images were subjected to thresholding and binary masks were generated. The binary mask was then used in integrated morphometry analysis to measure the average intensity of the population of U2OS cells expressing the RII β :Cat α IFP PCA. For dose-response measurements of the agonist, isoproterenol, cells were randomly identified as regions, and the average intensity of the cells before and after 15 min of addition were tabulated, followed by background subtraction²⁸. Deconvoluted data were further analyzed using GraphPad prism 6.0 for determination of half-life of RII β :Cat α complex and EC₅₀ of isoproterenol.

To study the SHC1-GRB2 interaction dynamics, we cotransfected pLpCSHC1-IFP-F[1] + mPlum and pLpCGRB2-IFP-F[2] + Venus YFP plasmids using TransIT-HeLaMONSTER transfection kit (Mirus Bio) and incubated at 37 °C and in 5% CO₂ for 24 h. Next, the cells were serum starved overnight, followed by addition of 40 μM of biliverdin-HCl for at least 3–4 h before imaging in DMEM minus phenol red. Epidermal growth factor (EGF, Cell Signaling) was added to cells at 20 ng ml⁻¹. Imaging of the cells was performed using InCell Analyzer 6000 using a Cy5.5 emission filter (excitation, 642 nm; emission, 725/50 nm) with an integration time of 500 ms, and images were captured before and after addition of EGF ligand at time points ranging from 1 to 49 min. Images were processed as stated previously. For quantification of fluorescence intensity, a binary mask was created for cells expressing the SHC1-GRB2 IFP PCA reporter using the Venus YFP as a cell marker for each time point; and as previously stated, integrated morphometry analysis was used to quantify the average fluorescence intensity of the cells over time before and after addition of EGF. To identify whether SHC1-GRB2 complexes are being compartmentalized in endosomes, we added 75 nM lysosomal marker (LysoTracker Red DND-99, Life Technologies) at least 30 min prior to imaging using a dsRed emission filter (excitation, 561 nm; emission, 605/52 nm), and cells were imaged before and after addition of EGF at 20 ng ml⁻¹ (ref. 29). The cells were maintained at 37 °C throughout the experiment. The human cell lines (HeLa and U2OS) used in this study were obtained from the University of Montreal, Department of Biochemistry, tissue culture facility, where the cell lines are regularly tested for mycoplasma contamination.

Spatiotemporal localization of Ste5-Fus3 complexes.

Recombinant strains of STE5 tagged with IFP-F[2] and FUS3 tagged with IFP-F[1] were obtained as described previously (“Construction of plasmids and cassettes”). One colony of strain Ste5-Fus3-IFP PCA was isolated to inoculate freshly prepared YPD medium with hygromycin-B (300 $\mu\text{g ml}^{-1}$), Clonat (100 $\mu\text{g ml}^{-1}$) and biliverdin-HCl (4 $\mu\text{g ml}^{-1}$) and incubated overnight at 30 °C. This overnight culture was used to inoculate fresh medium with the same composition to OD₆₀₀ of 0.05, as recommended elsewhere¹⁹. The culture was incubated at 30 °C with shaking at 200 r.p.m. for 2.5 h to reach an OD₆₀₀ of 0.1. To induce the pheromone pathway, we treated the culture with 10 μM α -factor diluted with 0.1 M ammonium acetate, and the same volume of 0.1 M ammonium acetate was added to the control cells without

pheromone treatment. Cells were attached to clear glass-bottom, black-walled microtiter plates by treatment with 0.1% concanavalin A and MnSO_4 as described elsewhere¹⁹. Differential interference contrast (DIC) images were acquired on a NIKON eclipse TE2000-U inverted microscope connected to a CoolSNAP-fx charge-coupled device (CCD) camera (Photometrics) using a 60× 1.5 DIC H Plan APO oil objective. To detect Ste5-Fus3 complexes, we used fluorescence microscopy with a band-pass Cy5.5 filter (specifications: scan range 600–800 nm, HQ665/45x, HQ725/50m Q695LP). Image analysis was performed with MetaMorph software (Molecular Devices). In order to distinguish the original signal from background, we thresholded the images and then filtered the results on the basis of the object size given in pixel counts. In this way, we were able to discriminate the foci formed by the Ste5-Fus3 complex from any other background signal. A strain expressing only Ste5-IFP-F[2] was used as negative control for this experiment. In order to image a larger cell population, we performed imaging of the cells using InCell Analyzer 6000 with a

Cy5.5 emission filter (excitation, 642 nm; emission, 725/50 nm) and integration time of 6,000 ms. Images were captured with and without addition of α -factor at time points ranging from 5 to 15 min. Images were processed as stated previously.

21. Kostecki, J.S., Li, H., Turner, R.J. & DeLisa, M.P. *PLoS ONE* **5**, e9225 (2010).
22. Sambrook, J.F. & Russell, D.W. *Molecular Cloning: A Laboratory Manual* 3rd edn. (Cold Spring Harbor, 2001).
23. Goldstein, A.L. & McCusker, J.H. *Yeast* **15**, 1541–1553 (1999).
24. Auldridge, M.E., Satyshur, K.A., Anstrom, D.M. & Forest, K.T. *J. Biol. Chem.* **287**, 7000–7009 (2012).
25. Chen, D., Brown, J.D., Kawasaki, Y., Bommer, J. & Takemoto, J.Y. *BMC Biotechnol.* **12**, 89 (2012).
26. Anand, G., Taylor, S.S. & Johnson, D.A. *Biochemistry* **46**, 9283–9291 (2007).
27. Serrano, M., Lin, A.W., McCurrach, M.E., Beach, D. & Lowe, S.W. *Cell* **88**, 593–602 (1997).
28. Zaccolo, M. *et al. Nat. Cell Biol.* **2**, 25–29 (2000).
29. Di Guglielmo, G.M., Baass, P.C., Ou, W.J., Posner, B.I. & Bergeron, J.J. *EMBO J.* **13**, 4269–4277 (1994).